Analysis of a Sole-Profile Definition in an Ankle Foot Orthosis Device

Eduardo F. Vazquez-Santacruz
Departamento de Ingeniería Eléctrica
Universidad Autónoma Metropolitana
Ciudad de México
evazquez.santacruz@izt.uam.mx

J.A. Vazquez-Santacruz
Facultad de Ing. Eléctrica y Electrónica
Universidad Veracruzana
Boca del río, Veracruz
alejanvasquez@uv.mx

Rogelio de J. Portillo-Vélez
Facultad de Ing. Eléctrica y Electrónica
Universidad Veracruzana
Boca del río, Veracruz
rportillo@uv.mx

***Resumen*—In this document, the human walking of a sane patient is considered in order to define a sole-profile which renders a natural dynamic walking pattern for an ankle foot orthosis (AFO) sole-geometry. In order to define the sole-profile, some characteristics are derived from the walking cycle from the perspective of two models emulating the legs of a human while walking. The models differs one from anther in the number of degrees of freedom (DOF) which are developed to obtain the dynamic support along the gait and verify the effect of the ankle joint, which could be disable under the AFO usage. The first approach considers then 4-DOF model, with ankle disabled, while the second approach considers a 8-DOF structure by considering a limited ankle joint rotation. The performed analyzes produce four different sole designs that have been analyzed for the manufacturing of prototypes from CAD models, which might be adapted for the requirements of each patient.**

I. Introduction

Among several treatment methods of ankle fracture, orthosis design has been focused in strategies to protect damaged regions, [1]. However, the selection of the appropriate AFO for a given user must consider several factors to provide comfort and security.

AFOs have been widely studied for fracture treatment, [2]. Recently, comfort and adaptability in AFO design has been addressed by researchers [3]. In order to develop an orthosis device by means of a CAD/CAM, a three dimensional analysis of a foot sole surface model system has been reported, [4]. A similar definition allows to simulate an AFO performance is presented in [5]. The sole profile is associated with the gait, as presented in [6], where the variation of the pressure and stress distribution in the foot surface is numerically modeled. The interaction of an AFO and the foot is optimized along the walking cycle, by minimized the stress at the sole with a specific geometry, [7]. The pressure at the sole is also addressed in [5], where the function of the toes produces a 3D AFO model. The parameters involved in the sole-profile design require methods to be characterized in order to evaluate their impact in the final geometry. In a closer work to ours, a stiffness measurement device is validated from an AFO during the reproduced gait into the sagittal plane, [8].

In order to explore a sole-geometry profile that allows a natural anatomical performance for an AFO, in this work, it is addressed the walking cycle performance with focus on a natural dynamic foot support. Since an AFO is generally described by a rigid device, it normally produces an user-uncomfortable walking. Therefore, it is desirable to provide the device with some characteristics that overcome this trouble and to reproduce a natural rotation at the sole surface as developed by a healthy ankle. The sole profile is thus defined from an exploration of the effect of the center of mass of the user during gait, and the analysis is done by means of some structural approaches in order to virtually reproduce the natural dynamic walking cycle while using an AFO.

The paper is structured as follows. In Section II, the problem of an adequate sole profile is addressed for the design of ankle foot orthoses. To render a sole-profile, different approaches based on the walking cycle are addressed in Section III. In Section IV, a discussion of the results is presented. Some conclusions are drawn in Section V.

II. Problem definition

Since an AFO is in general a rigid device, it eventually forces the foot to move in an unnatural way, thus producing an uncomfortable walking for the user. It is then necessary to provide an anatomical performance to the walking; the main contribution of this paper aims to render it by means of a specific sole-profile. This is very important in the AFO design, not only because of the rotation but also because of the foot length. To the best of authors knowledge, this represents a pioneering study of the sole profile for AFO design while recent works mention its relevance [9].

A kinematic analysis of a structural device that emulates the human body during the gait is developed in order to explore a relation between a center of mass of the body and the ground through a sole definition profile. By knowing the center of mass evolution during the gait, it is assumed that a natural sole profile is deduced at the lateral plane. Since the real center of mass evolution of the human body is not monitored, an anthropomorphic structural model is explored and simulated in order to analyze the possible described relation. It is assumed that the third dimension is homogeneous since it is desirable to maintain the foot as vertical as possible during the gait.

978-1-6654-5508-4/22/$31.00

III. Methodology for sole profile analysis

In this section, an exploration of relevant characteristics of the human walking cycle by means of two structural approaches of a biped locomotion system related to the problem definition is presented. Both approaches render a solution for a sole profile definition, tough using different DOF in the analyses, which might render optimization of the sole profile for a given criteria in further studies. The main idea of the geometry definition starts from the need to rotate at the a standing foot during the walking when the ankle joint is disabled, so that a first approach of a 4-DOF model is presented in section III-A. Though the orthosis is defined with an anthropomorphic design to be adapted to the extremity, the main results of this analysis focuses on providing stiffness to the lower joints.

In section III-B, an exploration of the center of mass of the model during a particular gait allows to define its effect on the sole and an specific geometry profile rotation overcomes the required natural ankle joint and an 8-DOF model is also addressed.

In section IV, the results are compared and a simple and natural profile is obtained for a latter experimental validation which is out of the scope of this paper. Each model is numerically studied and renders a sole proposal with a sole profile that is finally implemented in the AFO design. In a practical implementation the soles are intended to be exchangeable or user defined according to the walking performance for each patient.

III-A. A 4-DOF model for gait cycle

For the first walking analysis, it has been considered a simple 4-DOF approach to define a biped locomotion. In this way, it is considered a two leg system with hip and knee joints. The model is showed in Fig. 1, where the the joints and limbs are depicted.

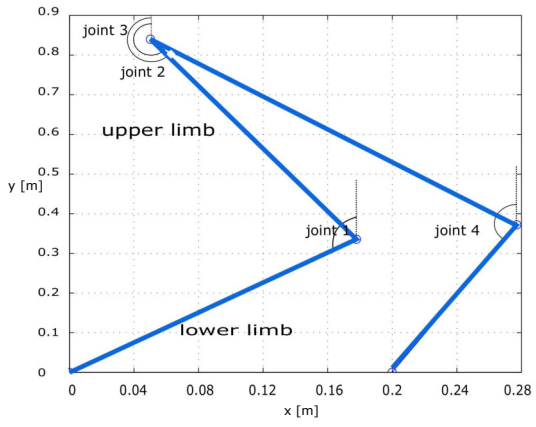

Figura 1: 4 DOF model for walking analysis

The analysis is based on the knowledge of the joint positions $P_i = (X, Y)$, related to the hip and knee, which are derived from a direct kinematics by considering the base point $P_0 = (X_0, Y_0)$ at the stance foot ending. The join points are located as:

$$X_{k1} = X_0 + L_2 cos(\theta_1) \qquad X_{k2} = X_h + L_2 cos(\theta_{123})$$
$$Y_{k1} = Y_0 + L_2 sin(\theta_1) \qquad Y_{k2} = Y_h + L_2 sin(\theta_{123})$$

$$X_h = X_{k1} + L_1 cos(\theta_{12}) \qquad X_{sf} = X_{k2} + L_1 cos(\theta_{1234})$$
$$Y_h = Y_{k1} + L_1 sin(\theta_{12}) \qquad Y_{sf} = Y_{k2} + L_1 sin(\theta_{1234})$$

where L_1 and L_2 are the length of the upper and lower limb respectively. Notice that the joint angles $\theta_i,\ i = 1, 2, 3, 4$ are defined with respect to the vertical reference. The notation is simplified such that $\theta_{ij..m} = \theta_1 + \theta_2 + ... + \theta_m$ and the sub-index $k1$, $k2$, h and sf describe the supporting knee, the swing knee, the hip and the swing foot position respectively.

To introduce the procedure of sole profile definition, consider a first approach to describe a relation between stand foot and the center of mass of the robot during the walking cycle. In order to do this, a biomechanical analysis determines the center of mass by means of distal (X_D, Y_D) and proximal (X_P, Y_P) points as well as their location in any limb of the human body. In Fig. 2 it is shown the distribution of the center of mass according to these points, where $P_D = (X_D, Y_D)$ as distal point is the farthest connection point and, $P_P = (X_P, Y_P)$ as proximal is the closer connection point.

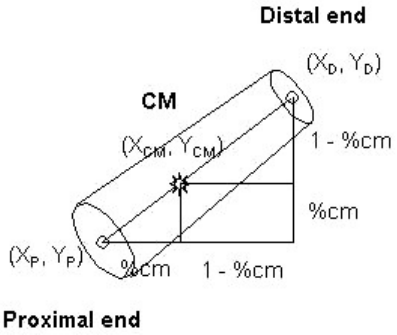

Figura 2: Center of mass locations

The anatomy of the human body is such that a thigh as the upper limb of a leg has the hip as proximal point and the knee as distal point. Similarly, the lower limb of the leg has the knee and the foot as proximal and distal points respectively.

Regarding both limbs, the calculation of the center of mass has been analyzed from samples in a generalized population, in congruence with [10], where a mean value locates the CM at 40 % from the proximal point at the thigh and at 43 % for the lower limb as depicted in Fig. 2, where it is also depicted the total robot center of mass CM.

In order to become more realistic, see Fig. 3, it has been incorporated an extra element of the approach emulating

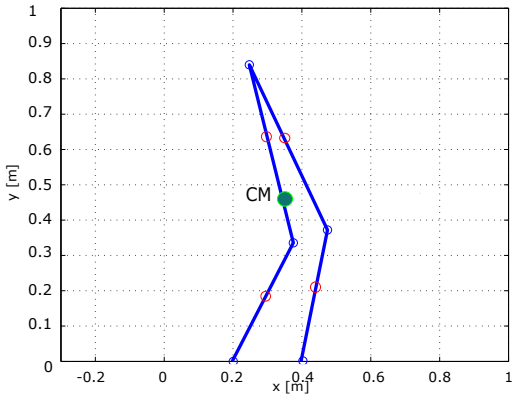

Figura 3: Legs center of mass locations

the torso with mass and dimensions according to the population in [11], that induces the total center mass located at (X_{CMT}, Y_{CMT}) and defined as:

$$X_{CMT} = \frac{\sum m_i X_i}{\sum m_i} \qquad Y_{CMT} = \frac{\sum m_i Y_i}{\sum m_i}$$

where m_i correspond to the mass of each element including torso.

The overall approach is depicted in Fig. 4 where clearly the CMT point is modified compared with the simple CM of the model without torso.

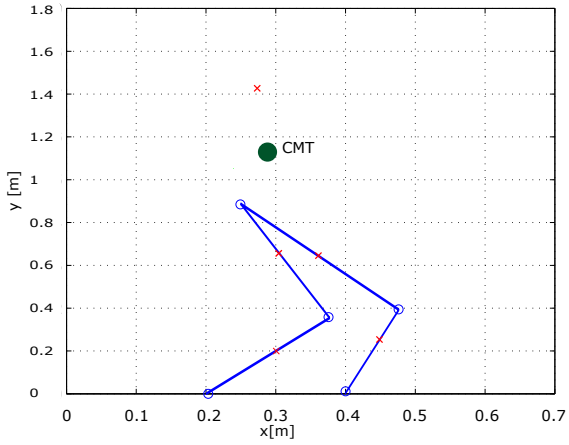

Figura 4: Center of mass of the 4 DOF model

III-A1. Analysis I, distance from the CMT to the supporting point: Based on the 4-DOF approach, a first analysis studies an anthropomorphic gait cycle monitoring the CMT performance with respect to the supporting point at the stance leg. For the analysis, they are considered mass and lengths for the limbs of a standard person as [11], [12], such that the thigh is taken as 41 [cm] and 7 [kg]; and 40 [cm], with 4 [kg] for the lower limb.

Based on the model in Fig. 4, it is obtained the distance $V = [V_x, V_y]^T$ between the center of mass of the body (X_{CMT}, Y_{CMT}) and the supporting point at the stance leg in (X_0, Y_0). In this way, it is possible to define,

$$V_x = X_{CMT} - X_0, \qquad V_y = Y_{CMT} - Y_0$$

However, since the effect of the CMT is studied along the standard size of the foot of 27 (cm), in Fig. 5 it is observed how the x-component evolves in distance along this standard size. This variation allows to infer a geometry since the closer the CMT, the higher the effect of the mass in the support and the sole has to compensate it with a higher thickness.

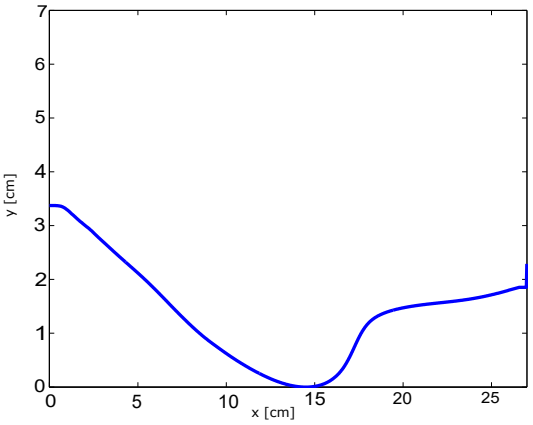

Figura 5: Distance evolution from CTM to the support point during gait

According to this, to design a first approach of the sole geometry, it has been taken the maximal distance of the convex section of the performance in the figure to define the maximal thickness in the corresponding location along the foot and, following this, a possible sole profile is defined such that the heel starts at the zero position 0 (cm), the maximal convex point at 3.37 (cm) and the tiptoe at 1.85 (cm). In Fig. 6, it is shown the derived geometry of the sole profile from the mapping from a lateral view.

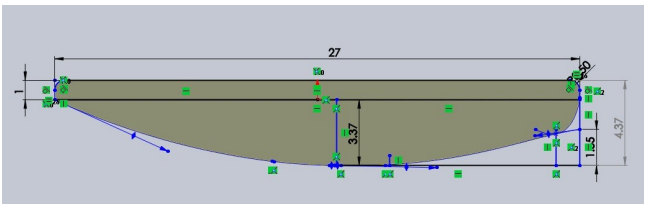

Figura 6: Lateral view of the preliminary sole

III-A2. Analysis II, ground reaction force from the CMT: Since the previous analysis is fully geometric, it is natural an analysis to find a relation between the reaction force in the supporting during the walking along the foot, such that its magnitude could be evaluated along the gait as a function of the curvature of the sole.

In order to develop the analysis, the reaction force F is derived from the displacement of the total center of mass CMT, and the acceleration of the associated mass (a_{cmx}, a_{cmy}) from the time varying dynamics of the gait. By considering the total body mass M_T, it is obtained the components of the force F as follows:

$$F_x = M_T a_{cmx}, \qquad F_y = M_T a_{cmy}$$

In Fig. 7 it is possible to analyze the performance of the reaction force at the supporting point with respect to the walking cycle dynamics. The reaction force is derived as a decomposition of the total force on the equivalent mass that is produced by the acceleration. In order to know that force, the angles α and β depicted in Fig. 7 are required, and they are derived by means of geometrical tools.

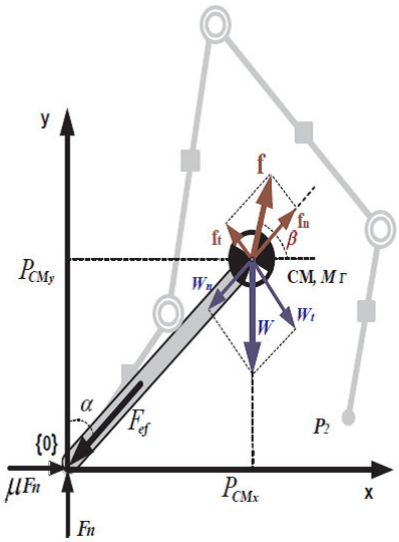

Figura 7: Reaction force at the supporting point

In this way, the effective reaction force at the support is obtained as $F_{ef} = Wn - Fn$, with $Wn = Wcos(\alpha)$ and $Fn = Fsen(\alpha + \beta)$, being W the total weight and F the force due to the acceleration.

The analysis of the force and the associated sole profile is derived from these equations and, by discriminating the transitory impulses, it can be deduced a similar performance of the first analysis. The performance of the reaction force can be observed in Fig. 8, notice that along the standard size foot of 27 (cm), the maximal force is present where the body is in the vertical position and the lower distance from the center of mass is present.

This analysis is only valid along the foot and it is developed a transformation between the force magnitude in Newtons and the maximal distance in centimeters derived from the first analysis, it is 3.37 (cm), see Fig. 9.

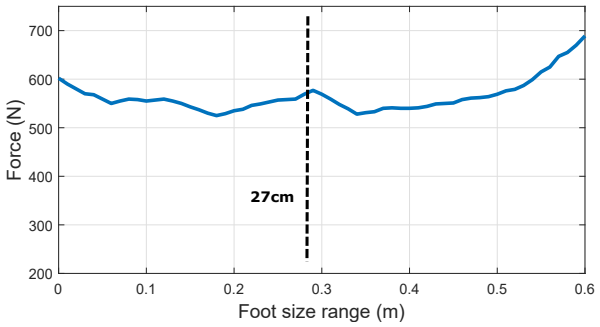

Figura 8: Bounded reaction force

The result of the geometry projection allows to locate the support point of the sole as depicted in Fig. 9 with a lateral view and advance direction to the left.

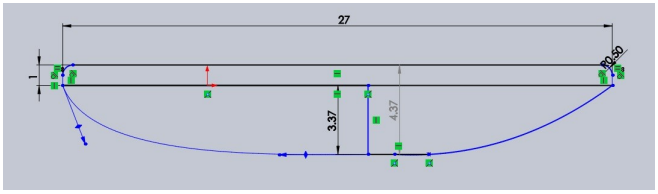

Figura 9: Lateral view of the sole design

III-B. An 8-DOF model for gait cycle

For the second model analysis, it is considered a similar structure but additional degrees of freedom are incorporated such that the tiptoe, the foot, the lower limb and the thigh integrates a full model for the leg. In this case, the model consists in 8 limbs and joint-connection points at hip, knees, ankles and toes as depicted in Fig. 10 with small circles.

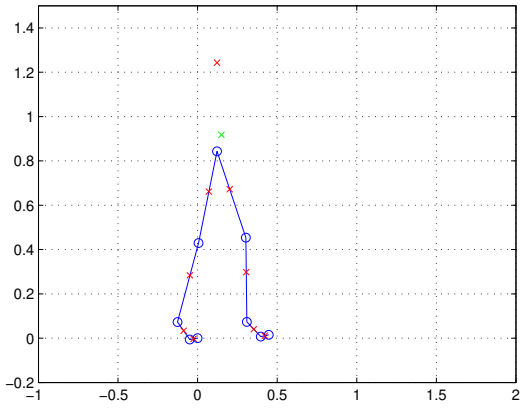

Figura 10: An 8DOF model

By considering the tiptoe fixed at $[x_0, y_0] = [0, 0]$, the location of the joints in the model is derived from a kinematic analysis as:

$$
\begin{aligned}
x_1 &= d_1 cos(\theta_4) & x_5 &= x_4 + d_4 cos(\theta_5) \\
y_1 &= d_1 sen(\theta_4) & y_5 &= y_4 + d_4 sen(\theta_5) \\
x_2 &= x_1 + d_2 cos(\theta_3) & x_6 &= x_5 + d_3 cos(\theta_6) \\
y_2 &= y_1 + d_2 sen(\theta_3) & y_6 &= y_5 + d_3 sen(\theta_6) \\
x_3 &= x_2 + d_3 cos(\theta_2) & x_7 &= x_6 + d_2 cos(\theta_7) \\
y_3 &= y_2 + d_3 sen(\theta_2) & y_7 &= y_6 + d_2 sen(\theta_7) \\
x_4 &= x_3 + d_4 cos(\theta_1) & x_8 &= x_7 + d_1 cos(\theta_8) \\
y_4 &= y_3 + d_4 sen(\theta_1) & y_8 &= y_7 + d_1 sen(\theta_8)
\end{aligned}
$$

where d_1 is the limb length given by the toes, d_2 the foot length, d_3 the lower limb length and d_4 the thigh length.

III-B1. Analysis III, distance from the ankle joint to the tiptoe: In this analysis it is developed a relation between the performance of the articulated foot and the sole profile. Since the sole is tightly related with the support, they are analyzed three joint points at the foot defined by the tiptoe ($P_0 = [x_0, y_0]$), toes ($P_1 = [x_1, y_1]$) and ankle ($P_2 = [x_2, y_2]$) for the supporting leg as depicted in Fig. 11.

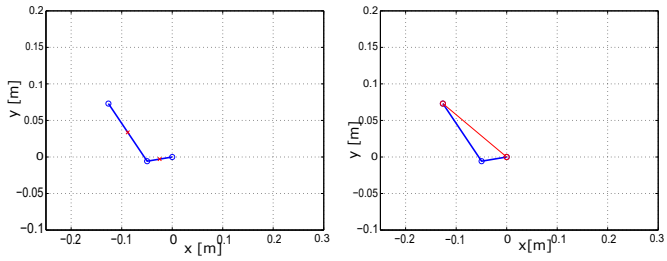

Figura 11: Foot: ankle joint and toes

Since the ankle is assumed to be at a constant distance from the heel, the magnitude of the linear segment from tiptoe to the ankle, depicted in a red line in Fig. 11, will provide information of the rotation dynamics during the walking on the supporting foot. Let define D, the magnitude of this distance between the ankle to the tiptoe, then it is defined as,

$$D_x = x_2 - x_0 \qquad D_y = x_2 - x_0$$

The magnitude of $1D1$ on the supporting foot is plotted during the first step in the walking. From 200 samples that represent the total step where the stance leg becomes the support again according to [10], it is analyzed only the half of samples, related with the single supporting foot cycle, a half gait. The result is depicted in Fig. 12.

Notice that the magnitude, $|D|$, varies between 137 (cm) and 156 (cm), that serves as bounds for a standard size of 27 (cm). With this variation, punctual magnitudes are sampled during the half gait, and they are traced starting from the heel and the tiptoe, and ending each in a common point over the sole. The circular profile derived from the above observation serves as a sole-profile definition, as depicted in Fig. 13.

Since the height of a standard ankle from heel is about 11 (cm), at that location is traced the first magnitude of 13.76 (cm) and the last one of 14.56 (cm) is associated with the tiptoe. which represent the extremal magnitudes along the foot. This is depicted in Fig. 13, where it can be noticed that the

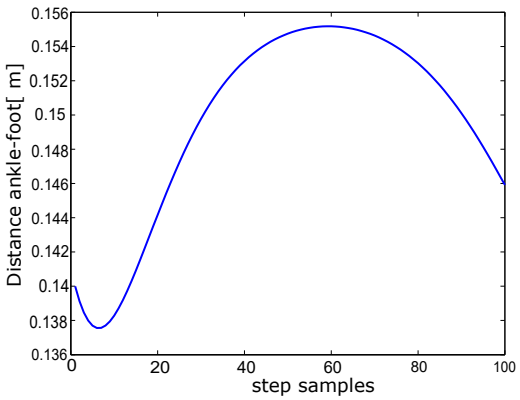

Figura 12: Distance from the ankle to the tiptoe $|D|$

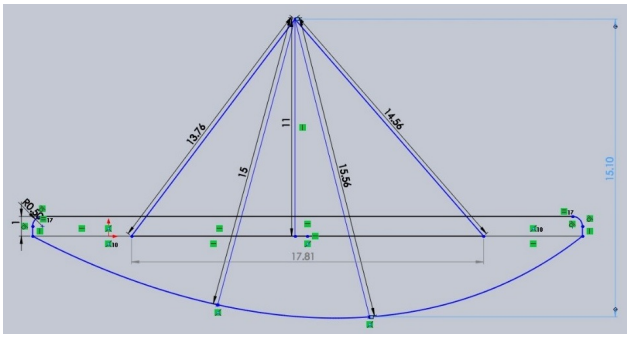

Figura 13: Lateral view of the profile, units in (cm)

geometry of this segments describes an effective area of the sole along 17.8 (cm) that is extended along the standard foot of 27 (cm). The effective length allows to trace the maximal magnitude of 15.66 (cm) by using the references of the Fig. 12 in order to know the slope of the segment and reproduce a sole geometry.

III-B2. Analysis IV, distance from the bounded supporting point: In this analysis, the performance of the foot is derived from analysis III. Based on Fig. 12, the difference between the minimal and maximal amplitudes can be computed and then the performance is scaled with this bound. The resulting maximum amplitude is 1.76 (cm) that is distributed along the standard foot of 27 (cm), the profile is depicted in Fig. 14.

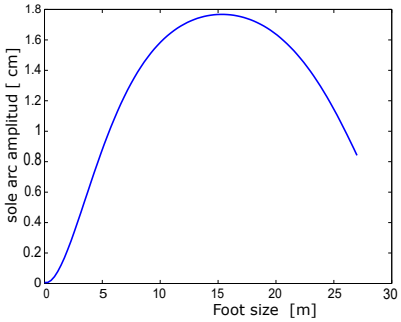

Figura 14: Bounded distance foot-ankle

By using the sole profile of Fig. 14, it is defined the sole design from the vector norm. The design is showed in Fig. 15, where a lateral view is depicted with a maximal amplitude of 1.76 (cm) located at 16 (cm) from the heel.

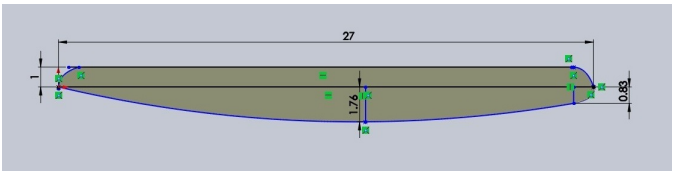

Figura 15: Lateral view of the sole profile

IV. Results analysis

The resulting sole-profile geometries are derived from similar conditions.To analyze the real performance of each sole-profile proposal they have to be manufactured as sole prototypes and evaluate their impact in comfort and stress for the user. For this paper a CAD model of the AFO was developed in order to show the physical implications of the use of the obtained sole-profile, see Fig. 16. Though the approach of the 8-DOF structure reproduces the biomechanical dynamics in a more realistic situation, it has been noticed that the 4-DOF model with the *Analysis II* that incorporates the reaction force, produces a sole profile that might provide better adjust to the extremity and produce a stability and security sensation in the user, this is an expected result since an AFO user is set to develop an ankle disabled dynamics; however, this observation must be confirmed by future experimentation.

In Fig. 16 it is depicted the assembled orthosis device incorporating the sole profile derived from the *Analysis II*. Some different perspectives are shown in a full virtual CAD prototype device. As already mentioned, the sole is defined to be exchangeable according to the sole that better adapts the patient conditions. Notice that it has been adapted an insertion pattern that allows to the sole to be rigid in the device.

Figura 16: Perspectives of the device

V. Conclusion

The analysis of this work have explored some approaches and their relation with a possible sole-profile for an AFO design. Though all defined profiles have been oriented to circular shapes because of the required rotation, it has been detected a natural relation of the geometry from different dynamical perspectives. It has been expected that an increasing characteristic incorporation provide a sole-profile that better adjust to the natural walking cycle. However, an important issue to be evaluated as the comfort of the user, determines that a simple model approaches may be enough to define a sole-profile that has been currently adapted to ankle fracture therapy with a particular AFO. In this context, it is important to highlight that the scope of this paper aims to provide a sole profile design while its manufacturing is considered as future work, which will be helpful to render sharpen conclusions of our approach.

Referencias

[1] R. Singh, T. Kamal, N. Roulohamin, G. Maoharan, B. Ahmed, and P. Theobald, "Ankle fractures: A literature review of current treatment methods," *International Journal of Control, Automation and Systems*, vol. 2014, no. 4, pp. 292–303, 2014.

[2] D. N. Condie and C. Meadows, "Some biomechanical considerations in the design of ankle-foot orthoses," *Orthotics and Prosthetics*, vol. 31, no. 3, pp. 45–52, 1977.

[3] R. L. Lenhart and N. Sumarriva, *Design of Improved Ankle-Foot Orthosis*. University of Tennessee Honors Thesis Projects., 2008.

[4] P. O. Mogeni, "Design and development of a cad/cam system for foot orthotics," in *The Second International Conference on Technological Advances in Electrical, Electronics and Computer Engineering (TAEECE2014)*, 2014, pp. 90–99.

[5] J. Inoue, W. Yu, K. Kawamura, and M. G. Fujie, "A detailed 3d ankle-foot model for simulate dynamics of lower limb orthosis," in *Annual International Conference of the IEEE*, 2011, pp. 8141–8145.

[6] A. Gefen, M. Megido-Ravid, Y. Itzchak, and M. Arcan, "Biomechanical analysis of the three-dimensional foot structure during gait: A basic tool for clinical applications," *Journal of Biomechanical Engineering*, vol. 122, no. 6, pp. 630–639, 2001.

[7] N. Jamshidi, H. Hanife, M. Rostami, S. Najarian, M. B. Menhaj, M. Saadatnia, and F. Salami, "Modelling the interaction of ankle-foot orthosis and foot by finite element methods to design an optimized sole in steppage gait," *Journal of Medical Engineering and Technology*, vol. 34, no. 2, pp. 116–123, 2010.

[8] T. Kobayashi, A. K. Leungi, Y. Akazawa, H. Nait, M. Tanaka, and S. Hutchins, "Design of an automated device to measure sagittal plane stiffness of an articulated ankle-foot orthosis," *Prosthetics and Orthotics International*, vol. 34, no. 4, pp. 439–448, 2010.

[9] E. Wright and S. A. DiBello, "Principles of ankle-foot orthosis prescription in ambulatory bilateral cerebral palsy," *Physical Medicine and Rehabilitation Clinics*, vol. 31, no. 1, pp. 1047–9651, 2020.

[10] P. de Leva, "Adjustments to zatsiorsky-seluyanov's segment inertia parameters," *Journal of Biomechanics*, vol. 29, no. 9, pp. 1223–1230, 1996.

[11] A. Pichardo, J. Perez-Oribe, and D. Chavez, "Estudio de parámetros cinemáticos de la marcha normal en hombres adultos. estandarización para la población mexicana," *Revista Mexicana de Ortopedia y Traumatología*, vol. 12, no. 5, pp. 377–379, 1998.

[12] J. Perez-Oribe, A. Pichardo, and D. Chavez, "Desarrollo de un estandar de marcha normal en hombres adultos. propuesta de estándar para la normatividad en estudios de marcha de población mexicana." *Revista Mexicana de Ortopedia y Traumatología*, vol. 12, no. 5, pp. 380–385, 1998.